Sensors & Actuators: A. Physical 396 (2025) 117239

Contents lists available at ScienceDirect

Sensors and Actuators: A. Physical

journal homepage: www.journals.elsevier.com/sensors-and-actuators-a-physical

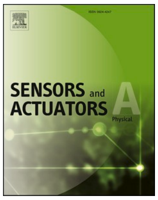

Reconstruction of the benzene absorption band at 14.8 μm in amplitude modulation exploiting a quartz tuning fork as optical detector

Andrea Zifarelli [a], Lavinia Anna Mongelli [a], Kumar Kinjalk [b], Alexei Baranov [c], Pietro Patimisco [a,d,*], Qijie Wang [e,f], Vincenzo Spagnolo [a,d], Angelo Sampaolo [a,d]

[a] PolySense Lab, Dipartimento Interateneo di Fisica, University and Polytechnic of Bari, Via Amendola 173, Bari 70126, Italy
[b] IES, University of Montpellier, CNRS, Montpellier 34095, France
[c] LAAS-CNRS, University of Toulouse, CNRS, France
[d] PolySense Innovations srl, Via Amendola 173, Bari 70126, Italy
[e] School of Electrical and Electronic Engineering, Nanyang Technological University, Singapore, Singapore
[f] Centre for Disruptive Photonic Technologies, Division of Physics and Applied Physics School of Physical and Mathematical Sciences, Nanyang Technological University, Singapore, Singapore

ARTICLE INFO

Keywords:
Light-induced thermoelastic spectroscopy
Quartz tuning fork
Gas detection
Benzene
Quantum cascade laser
Amplitude modulation
Wavelength modulation

ABSTRACT

This work presents a single-pass optical sensor designed for the detection of a broadband absorption feature of benzene. It is based on light-induced thermoelastic absorption spectroscopy (LITES) employing a novel InAs/AlSb-based quantum cascade laser source emitting at 14.85 μm as light source, and a custom-designed quartz tuning fork (QTF) as infrared photodetector. The sensor system was operated in both amplitude (AM) and wavelength modulation (WM) mode to characterize the absorption band parameters and assess the sensor ultimate detection limit. The limitations of WM and double-frequency detection (2f-WM) approach for broadband absorption features are thoroughly analyzed and discussed. An absorption cross-section of $(1.1 \pm 0.1) \cdot 10\ \mathrm{cm}^2$ was measured in AM mode with a minimum detection limit of 1.6 part-per-million, while a minimum detection limit of 0.6 part-per-million was achieved using the 2f-WM mode, at 0.1 s of integration time, employing a 12 cm long single-pass cell.

1. Introduction

Optical absorption spectroscopy has proven to be a valuable technique due to its ability to distinguish among different substances with a high accuracy by reconstructing the related absorption features. Diode laser sources have been widely employed in direct absorption configuration, comparing the residual radiation intensity with and without the target analyte, in accordance with the well-known Lambert-Beer law. Additionally, they offer the distinct advantage of wavelength tunability through injected current. However, by implementing modulation techniques such as amplitude and wavelength modulation, high detection sensitivities can be achieved when they are combined with low-noise demodulation approaches [1,2]. In Amplitude Modulation (AM) spectroscopy, the laser is switched on/off at a fixed modulation frequency. When only the spectral component ν of the transmitted radiation I_T is extracted, for example using a lock-in amplifier, the ratio I_T/I_0 (where I_0 is the incident intensity) can be plotted as a function of the light frequency, namely the laser current. This plot follows the trend of the absorption coefficient $\alpha(\nu)$ just as in direct absorption spectroscopy, with the advantage of a significantly lower photodetector noise level thanks to the filtering of noise components outside a narrow bandwidth around ν. Therefore, the AM-based spectroscopic technique enables the full reconstruction of the spectral features; however it is not inherently background-free [3]. A viable alternative is a Wavelength Modulation (WM) approach [4]. In this case the laser injection current is modulated using a sinusoidal dither, resulting in a modulation of the laser emission wavelength as well as of the optical power [5]. The WM approach is usually combined with a double-frequency (2 f) demodulation of the photodetector signal. In the approximation of derivative spectroscopy, the reconstruction of the absorption feature will resemble the second harmonic derivative of the absorption coefficient $\alpha(\nu)$ without background signal [6–8]. A slight distortion typically appears as an asymmetry in the two lateral lobes, resulting from the contribution of Residual Amplitude Modulation (RAM), which is proportional to the

---

[*] Corresponding author at: PolySense Lab, Dipartimento Interateneo di Fisica, University and Polytechnic of Bari, Via Amendola 173, Bari 70126, Italy.
E-mail address: pietro.patimisco@uniba.it (P. Patimisco).

https://doi.org/10.1016/j.sna.2025.117239
Received 29 May 2025; Received in revised form 25 September 2025; Accepted 1 November 2025

optical power modulation induced by laser current modulation [9]. When detecting well-isolated, narrow absorption features associated with a single radiative transition, the choice is clear: 2f-WM is preferred over AM due to its background-free nature and typically higher signal-to-noise ratio. In such cases, the absorption feature's FWHM covers only a small fraction of the full dynamic current range of the laser source. Since the optimal amplitude of the sinusoidal dither is 1.1 times the FWHM, optical power modulation remains minimal, leading to a negligible RAM contribution. As a result, the absorption feature is accurately reconstructed as a second-derivative function of $\alpha(\nu)$, with minimal distortion from RAM. Additionally, the background signal (measured in the absence of absorbing species in the gas cell) appears spectrally flat, with an average value comparable to the noise level, eliminating the need for any post-processing subtraction.

In recent years, there has been a growing interest in detecting broadband gas species, characterized by spectral features which cannot be resolved even at fraction of atmospheric pressure (i.e., $P < 50$ Torr). In this scenario, the sensitive and selective detection of Volatile Organic Compounds (VOCs) is emerging as a major advancement in the field of gas sensing. Due to their high volatility (i.e., low boiling point), these compounds readily evaporate from products and surfaces into the air, leading to their widespread presence in various environments and posing significant risks to both the environment and public health [10,11]. Due to their inherent nature as heavy molecules, VOCs exhibit broadband absorption features, often deviating significantly from a Lorentzian lineshape. When applying WM techniques, what occurs in the case of broadband absorption features, where the FWHM spans nearly the entire dynamic current range of a laser source? While it is certain that AM remains unaffected, 2f-WM requires new considerations. To fully cover the absorption FWHM, the amplitude of the sinusoidal dither must be increased to the point where it becomes comparable to the total dynamic current range of the laser. Consequently, RAM increases, leading to significant signal distortion. In the extreme case, the characteristic second-derivative-like shape may no longer be recognizable, and consequently the selectivity can be negatively affected. Additionally, the RAM can become so significant that it could distort the background signal even in the absence of absorption, disrupting the expected zero-background condition [12–14].

To investigate this, we implemented both the AM and WM approach to reconstruct a broadband absorption feature of benzene located at 14.85 μm (674 cm^{-1}) in a standard laser-based absorption setup for gas sensing. Benzene was selected as a representative of BTEX, an important class of VOCs that also includes toluene, ethylbenzene, and o-, p-, and m-xylenes [15–17]. A long-wavelength InAs/AlSb Quantum Cascade Laser (QCL) was used to spectrally scan the selected absorption feature. Due to the lack of photoconductive, photovoltaic or thermal detectors capable of ensuring high detectivity at long wavelengths, a custom-designed T-shape Quartz Tuning Fork (QTF) was used as photodetector in a configuration known as LITES [18–23]. Thanks to its intrinsic ability to operate as a photodetector by converting photo-induced thermal energy in an electrical signal via the piezoelectric effect, the QTF is an ideal candidate for long-wavelength detection, as the selected wavelength falls within the spectral absorbance range of quartz [24]. A compact, single-pass cell with optical pathlength of 12 cm is placed between the laser source and the QTF-based photodetector to complete the LITES setup. The WM approach was implemented in the conventional way, by superimposing a sinusoidal dither onto the laser current while scanning across its dynamic range, investigating for the signal distortion arising from the requirement of large modulation depths, a consequence of the relatively broad FWHM of the benzene absorption feature. This approach was compared with an AM strategy. In this scheme, a square waveform is applied to the laser current, with a higher current level which was varied to scan across the absorption line, aiming to perform an accurate reconstruction of the spectral feature as well as a reliable retrieval of absorption parameters, with a high level of sensitivity.

2. Experimental setup

The experimental setup employed for benzene detection using the developed LITES sensor is sketched in Fig. 1.

An InAs-based long-wavelength QCL, designed to emit at $\lambda = 14.85$ μm to match the absorption band of benzene, was used as excitation source [25,26]. The laser beam was aligned through a 12 cm-long absorption cell equipped with two TPX windows with diameter of 40 mm and thickness of 2 mm and a pair of connectors for gas inlet and outlet. The radiation transmitted by the cell was focused on the QTF by means of a ZnSe lens with a focal length of 25 mm (THORLABS LA7542-E3).

The QCL source was driven using a THORLABS ITC4002, which allowed the control of both operating current and temperature. An external water chiller was used to help the Peltier cooler installed within the QCL package in efficiently dissipating the extra heat. A Keysight Edu33212A waveform generator was employed to generate a square wave or a sinusoidal dither, applied to the laser current driver for AM or WM operation, respectively. The QTF was mounted on a 5-axis stage to be aligned with respect to the incident laser beam. For both approaches, the modulated QTF signal was acquired using a custom transimpedance amplifier with feedback resistor $R_{fb} = 10$ MΩ and voltage gain of 30, to be then sent to a lock-in amplifier to be demodulated (Zurich MFLI). The lock-in integration time was set to 100 ms for all the collected measurements.

The gas line consists of two gas cylinders containing 240 part-per-million (ppm) of benzene in nitrogen (N_2) and pure N_2, as certified concentrations. A MCQ Gas Blender 100 was used to regulate the flow rate and generate gas samples with different concentrations of benzene in nitrogen. The operating pressure inside the gas cell was controlled using an Alicat MC3S-D pressure controller placed downstream of the gas cell, with its output connected with a membrane pump.

3. Characterization of the quantum cascade laser

The laser emission wavelength was measured using a Nicolet iS50 FTIR, mapping the source emission varying both the operating temperature and the injection current. This allows the evaluation of the optimal conditions to match the benzene absorption line at 673.95 cm^{-1}. In Fig. 2a, the wavelength is plotted as a function of the injection current, for two representative operating temperatures, T = -1°C and T = -5°C. In the same graph, the benzene absorption cross-section, simulated from the HITRAN database, is also provided [27].

The absorption feature of benzene can be fully reconstructed fixing the laser temperature at T = -1°C. The spatial quality of the laser beam profile was measured using a pyrocamera (Spiricon III HR Beam Profiling Camera) having an array of 160 × 160 pixels and a resolution of 80 μm, aligned to the laser beam. The beam profile was acquired by replacing the QTF with the camera in the setup of Fig. 1. It exhibits a

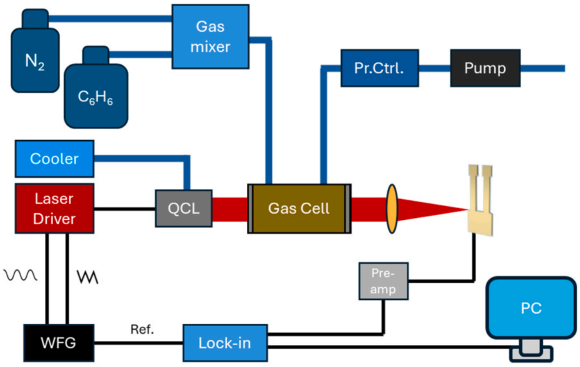

Fig. 1. Schematic of the experimental setup. Black lines indicate electrical connections, while blue lines mimic the gas tubes. Pr. Ctrl., pressure controller; PC, personal computer.

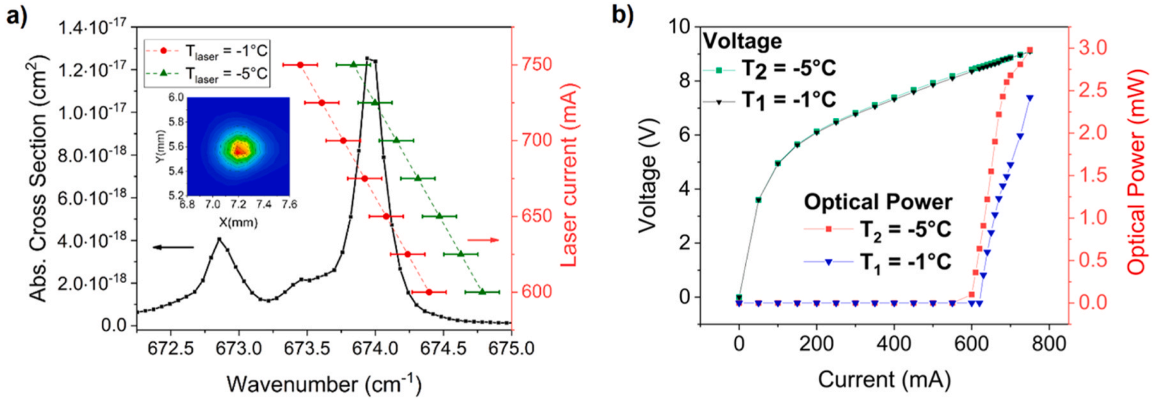

Fig. 2. (a) Benzene absorption spectrum simulated using HITRAN database at atmospheric conditions (black line). The right Y-axis reports the laser current matching the absorption feature at the operating temperature of −5 °C (green triangular datapoints) and −1 °C (red circular datapoints). The error bars represent the uncertainty associated to the FTIR resolution (0.125 cm^{-1}) (b) Laser LIV curve at the two representative temperatures: −5 °C (green and red squared datapoints) and −1 °C (black and blue triangular datapoint).

Gaussian-like, nearly circular profile with a diameter of ~500 µm along the x-axis and ~400 µm along the y-axis (inset Fig. 2a). The light-current-voltage curves of the QCL at the two selected temperatures are shown in Fig. 2b. A maximum power of 2.4 mW is reached when T = -1 °C.

4. QTF characterization

A custom T-shaped QTF was employed as infrared photodetector in the developed LITES sensor. The QTF consists of a hammer-shaped head with a length of 2.4 mm and a width of 2.0 mm, and a thinner prong body measuring 7.0 mm in length and 1.4 mm in width. The thickness of the QTF is consistent at 250 µm throughout. Additional information can be found in Ref. [18] where the same type of QTF is labeled as QTF-S08-T. The resonance properties of the QTF were measured by reconstructing the resonance curve of the fundamental in-plane flexural mode, at atmospheric pressure and room temperature, with an electrical excitation provided by the waveform generator. The resulting QTF signal, measured as a function of the input signal frequency, is shown in Fig. 3a, with y-axis values normalized to its peak value.

A Lorentzian fit was applied and superimposed to the collected data to evaluate both the resonance frequency and the quality factor, resulting f_0 = 12,460.7 Hz and Q = 14,700, respectively.

A 2D mapping of the LITES signal on the QTF surface was performed for identifying the point that maximizes the photo-induced electrical signal. The QTF was moved along both x and y axes on its plane with a step resolution of 0.3 mm in each direction, while the laser beam position remained fixed. The mapped area extends 4.2 mm along the x-axis and 2.4 mm along the y-axis. The results, presented as a color map in Fig. 3b, show that the highest LITES signal was detected in proximity of the prong base, where the maximum strain field is produced when the fundamental flexural mode is excited. This finding aligns with previous observations reported in literature [28].

5. Amplitude modulation detection scheme

The AM approach was implemented using a square wave function with a 50 % duty cycle, superimposed on the QCL injection current initially set to I_{DC} = 590 mA, below the lasing threshold. The lower voltage level of the square wave was fixed at 0 mV, while the upper voltage level was progressively increased to perform a complete scan of the absorption line. The square wave frequency was set to match the QTF resonance frequency (f_0 = 12,460.7 Hz), and the LITES signal was demodulated at the same frequency using a lock-in amplifier. The acquired signals were recorded at a lock-in integration time of 100 ms. The QCL was operated at T = -1 °C tuning the emission current in the range 610–750 mA. First, the benzene absorption feature was reconstructed at four different pressures, while the certified concentration of 240 ppm C_6H_6:N_2 flows in the gas cell. For the background acquisition, the same scan was acquired with pure N_2 flowing in the cell. The optical powers

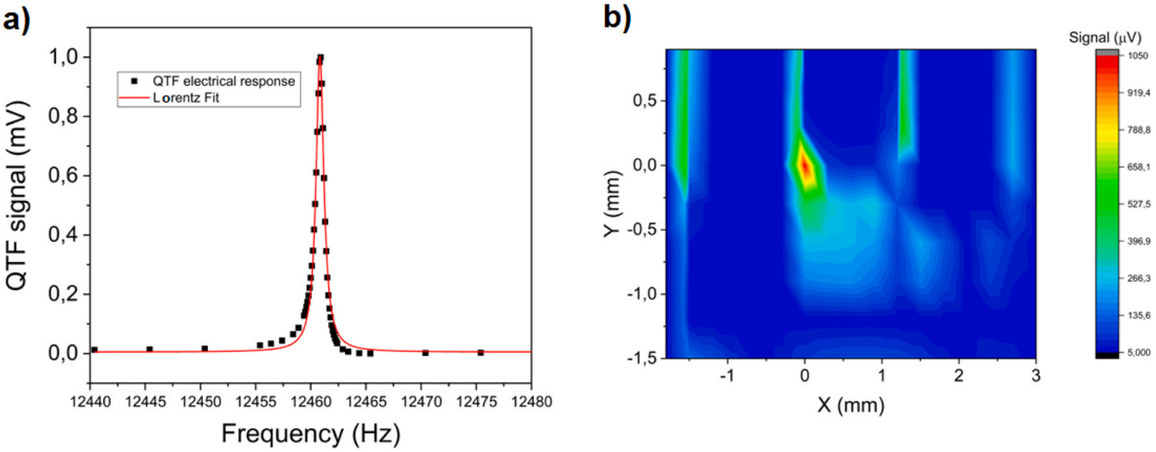

Fig. 3. (a) Normalized electrical response of the custom QTF used as photodetector (black dots). Lorentzian fit used to extract resonance frequency and quality factor (red line). (b) LITES peak signal mapping.

transmitted by the absorption cell are shown in Fig. 4a. The absorption feature of benzene is clearly observed as a dip, with a minimum around 690 mA, as expected. Below 630 mA, all curves overlap, confirming that no absorption occurs in this spectral region. Conversely, at higher injection currents beyond the absorption dip, the distribution of trends indicates the presence of an additional absorption contribution from benzene. As reported in Fig. 2a, this contribution can be easily attributed to the spectral overlap between the main feature peaked at 673.9 cm^{-1} and a secondary C_6H_6 absorption band around ~672.8 cm^{-1}.

The absorbance values A were calculated using the Lamber-Beer law, $A = ln\ (I_0/I_T)$, as the point-by-point ratio between I_T, the transmitted signal when benzene is present in the gas mixture and I_0, the background signal. The absorbance values as a function of the QCL injection current are plotted in Fig. 4b for the four investigated gas pressure values. The collected absorption profiles were fitted with a Lorentzian function, as expected at these pressure values, where molecular collisions in gas samples are the dominant mechanism of pressure broadening [29]. The highest absorbance intensity was observed at the highest gas sample pressure (P = 700 Torr), which reflects the highest number of benzene molecules in the gas cell.

The pressure has two opposite effects on the signal intensity: decreasing spectral line intensities due to pressure broadening and an increasing absorber number density with increasing pressure. According to Lambert-Beer theory, these two terms have the same but opposite dependence on pressure, thus should compensate. Fig. 4c shows the extracted peak absorbance as a function of the operating pressure, with a superimposed exponential, Lamber-Beer-like, fit:

$$y = y_0 \quad (1 - \exp(-A \bullet x)) \tag{1}$$

returning $y_0 = 1.07 \pm 0.04$ and $A = (1.98 \pm 0.15) \bullet 10^{-3}$ $Torr^{-1}$. The performed fit matches the experimental data with excellent agreement ($R^2 = 0.9996$), pointing out the emerging non-linearity. Indeed, at low pressures, the signal intensity linearly increases with pressure due to the increasing probability of light-sample interaction, as at very low pressure the absolute number of absorption molecule is low. At higher pressures, the effect of spectral broadening increases and the signal intensity approaches towards a plateau [29]. Fig. 4d shows the extracted Lorentzian halfwidth γ_L as a function of pressure, with a superimposed linear fit (R^2= 0.997). This linear trend aligns with the background theory, as the pressure broadening linewidth is known to scale proportionally with pressure [30].

The calibration of the LITES sensor was performed at an operating pressure of 700 Torr by acquiring spectral scans related to five dilutions

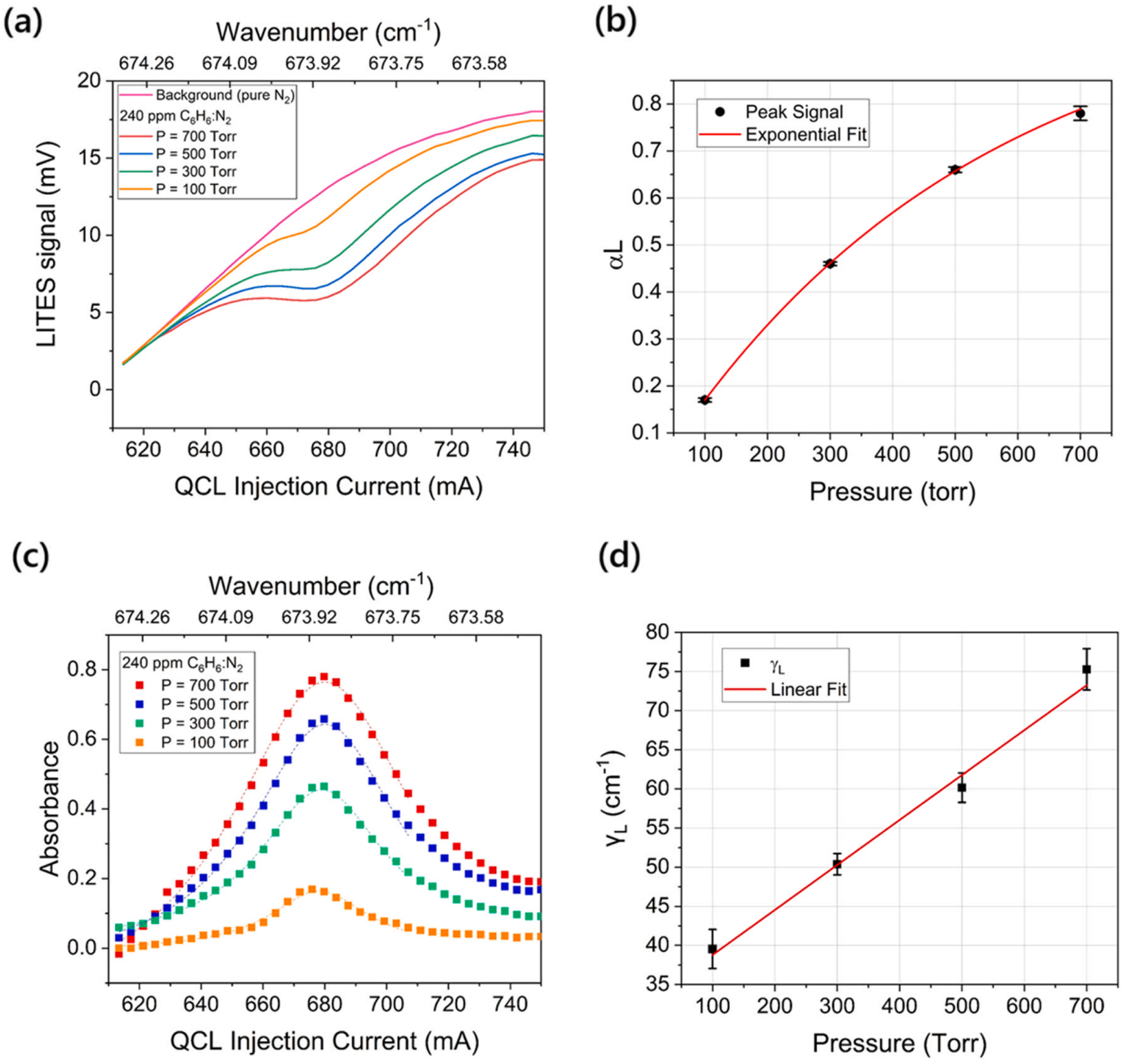

Fig. 4. (a) LITES 1f-AM spectral scans of the selected benzene absorption line at four different operating pressures, at QCL operating temperature T = -1°C. (b) Calculated benzene absorption coefficients at different operating pressures, fitted with Voigt function. (c) Peak values of the absorption profiles, plotted as a function of the operating pressure, and the corresponding best exponential fit. (d) Lorentzian halfwidth γ_L plotted as a function of the operating pressure fitted with a linear fit.

of the certified 240 C_6H_6:N_2 mixture in pure N_2, generated with the gas blender. As for the previous analysis, the absorbances were calculated using the Lambert-Beer law and plotted for different benzene concentration in Fig. 5a.

Peak values were extracted and plotted as a function of the benzene concentration in Fig. 5b. A sensitivity of 0.0034 ppm^{-1} was retrieved from the linear fit of the experimental data. The calibration curve was employed to estimate the minimum detection limit (MDL) of the LITES sensor. The MDL corresponds to the concentration at which the signal-to-noise ratio (SNR) equals 1. The noise level was defined as 1σ- fluctuations in the LITES signal when the upper level of the square wave was fixed, resulting in 0.05 mV for both benzene mixture and pure N_2 in the cell, which was then converted into absorbance fluctuations using the error propagation law. Based on this, an MDL of 1.6 ppm was estimated with a lock-in integration time of 100 ms. The absorbance measurements in Fig. 5a were further used to calculate the absorption cross section at the peak of the benzene band, applying the well-known relation:

$$\sigma(\omega) = A/(N_{tot} \bullet c \bullet L) \tag{2}$$

where $N_{tot} = 2.5 \cdot 10^{-19}$ was the molecular density of the sample, c was the gas target concentration and $L = 12$ cm was the measured optical pathlength. The calculated absorption cross section was $(1.1 \pm 0.1) \cdot 10^{-17}$ cm^2 corresponding to an absorption coefficient $(c = 1)$ $\alpha = N_{tot}\sigma = 270 \pm 21\ cm^{-1}$. The uncertainties associated to the retrieved values were calculated using the error propagation law.

The absorption cross section calculated from the experimental data was then compared with values available in the HITRAN [31] and GEISA [32] databases, as summarized in Table 1.

The experimentally measured absorption cross-section falls within the range of values reported in the HITRAN and GEISA databases. This agreement is particularly noteworthy, as it suggests that the experimental value represents a consistent and reliable estimation, in accordance with the adopted method.

6. Wavelength modulation detection

The 2*f*-WM approach was carried out by modulating sinusoidally the current of the QCL at a frequency $f_0/2 = 6230.35$ Hz using the waveform generator, while demodulating the QTF signal at $f_0 = 12{,}460.7$ Hz. The spectral scans of the benzene absorption band were acquired by adding a slow triangular voltage ramp at 5 mHz to the fast dither at $f_0/2$. The influence of gas pressure and modulation depth on the 2*f*-LITES signal was preliminarily investigated. Spectra of benzene absorption were obtained by varying the pressure inside the gas cell from 100 to 700 Torr, and the modulation depth from 100 to 700 mV. Representative spectra of benzene and nitrogen, measured at a modulation amplitude of 600 mV and a pressure of 700 Torr, are shown in Fig. 6a. The spectra were recorded by scanning the laser current over its full dynamic range. As predicted, the effect of extremely large modulation depth significantly impacts the accuracy of band reconstruction. The spectral scan acquired with benzene in the gas cell (red solid curve in Fig. 6a) deviates significantly from the expected second derivative of a Lorentzian function, with noticeable distortion in the negative lobes. This distortion arises from RAM contribution, which introduces a first-derivative component of the ultimate shape [33–35]. As a result, the negative lobe extends to the same degree as the positive lobe. Of course, the effect of this distortion increases with modulation depth, reaching its maximum at the highest investigated value, corresponding to a current modulation of 140 mA, comparable with the laser dynamic range. Moreover, at low injection currents, near the laser threshold, a non-zero signal was observed even in the absence of absorbing molecules. This was caused by optical power oscillations induced by the large modulation depth, i.e., again the RAM effect. Consequently, identifying a spectral interval with a true “zero signal” is not possible, complicating the determination of a reference for measuring the peak absorption value. The situation is even more problematic for the background signal, i.e., the spectral scan recorded with pure N_2 in the gas cell (black solid line in Fig. 6a). Unlike the ideal case of a spectrally flat background with a mean value within the 1σ noise level, as typically seen with a single narrow absorption feature, the background instead exhibits a distinct structure. With respect to flat, non-zero offset, the background subtraction results more challenging, also requiring continuous verification

Table 1
The absorption cross section calculated from the experimental data compared with the value obtained from HITRAN and GEISA databases.

	Experimental Value	HITRAN Database	GEISA Database
Absorption cross section [cm^2]	$(1.1 \pm 0.1) \cdot 10^{-17}$	$1.4 \cdot 10^{-17}$	$0.8 \cdot 10^{-17}$

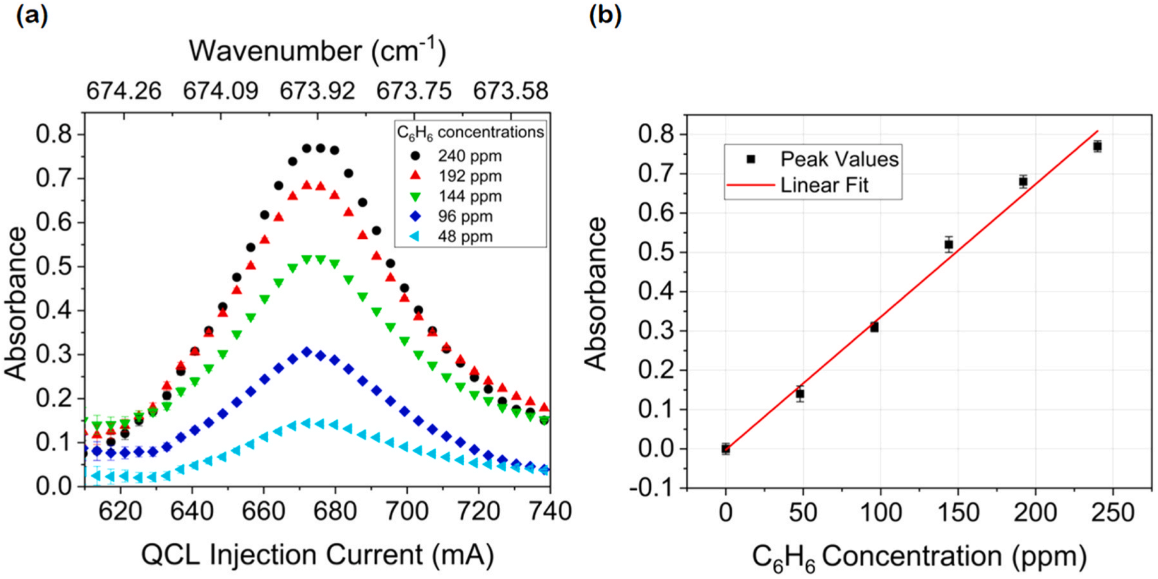

Fig. 5. (a) Absorbance of the benzene samples at different gas concentrations. (b) Peak values of the benzene absorption coefficients, at different concentrations, and the corresponding best linear fit.

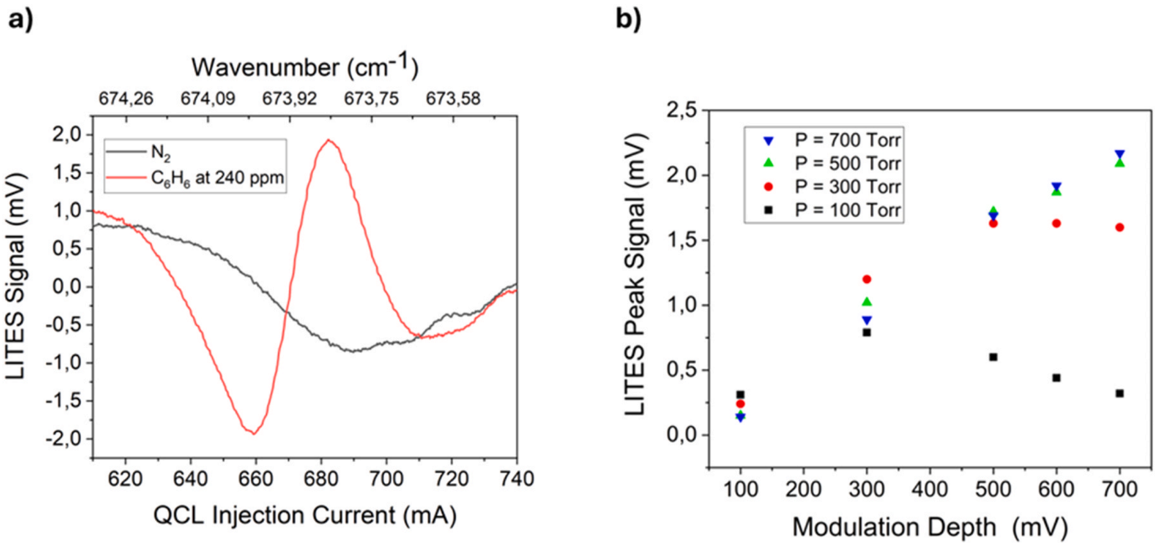

Fig. 6. (a) 2f-LITES spectral scan of the benzene (red line) and pure nitrogen (black line) absorption line at modulation depth of 600 mV and operating pressure of 700 Torr. (b) Peak values of the LITES spectral scans plotted as a function of different modulation depths at four different operating pressures.

to ensure long-term stability. As a result, the usual advantages of the 2f-WM approach are lost when dealing with large modulations targeting broad absorption features.

The peak values of the LITES spectra, recorded at different pressures, were plotted against modulation depths of the sine waveform applied to the QCL, as shown in Fig. 6b. For high pressure values, i.e., 500 and 700 Torr, the LITES signal increases monotonically, indicating that the maximum modulation depth used is insufficient to fully cover the broad FWHM of the benzene absorption feature. Higher modulation depths would be required, but their implementation is restricted due to the current limit imposed for laser safety. This behavior is expected at high pressures, as the FWHM increases with pressure, as observed in Fig. 4c. This not the case when the sensor operates at lower pressures, i.e., 100 and 300 Torr, where the two trends in Fig. 6b reach a maximum before decreasing at higher modulation depth values [36]. The highest LITES signal was achieved at 700 Torr with a modulation depth of 700 mV. However, to minimize signal distortion, a modulation depth of 600 mV was selected for further measurements, intentionally sacrificing a small fraction of the signal intensity to reduce the lineshape deformation. Consequently, all subsequent measurements were conducted at 700 Torr and 600 mV modulation depth. After identifying the optimal operating conditions, following the same approach as in the AM analysis, the *2 f*-LITES spectral scans were collected at different benzene concentrations, as shown in Fig. 7a.

The peak values of the LITES spectra were extracted and plotted against gas concentration in Fig. 7b, revealing a non-linear, exponential trend. The linear approximation of Lambert-Beer's law does not apply because of absorbance values approaching to 1, as observed using AM approach (see Fig. 5b). Moreover, the LITES peak signal at zero-benzene concentration differs from zero, as a consequence of the background pattern recorded in pure N_2 (Fig. 6a). Following the Lambert-Beer law, the experimental data in Fig. 7b were fitted using the exponential function shown in Eq. 1 with an additional offset contribution, B, to account for the non-zero offset. and the resulting fitting parameters were: $A = (0.053 \pm 3.8) \cdot 10^{-4}$ ppm^{-1}, $B = (-\ 0.74 \pm 0.03)$ mV, $y_0 = (3.8 \pm 0.15)$ mV, with $R^2 = 0.9995$.

Due to the non-linear sensor's response, its sensitivity varies with the concentration and can be calculated as the slope of the tangent to the

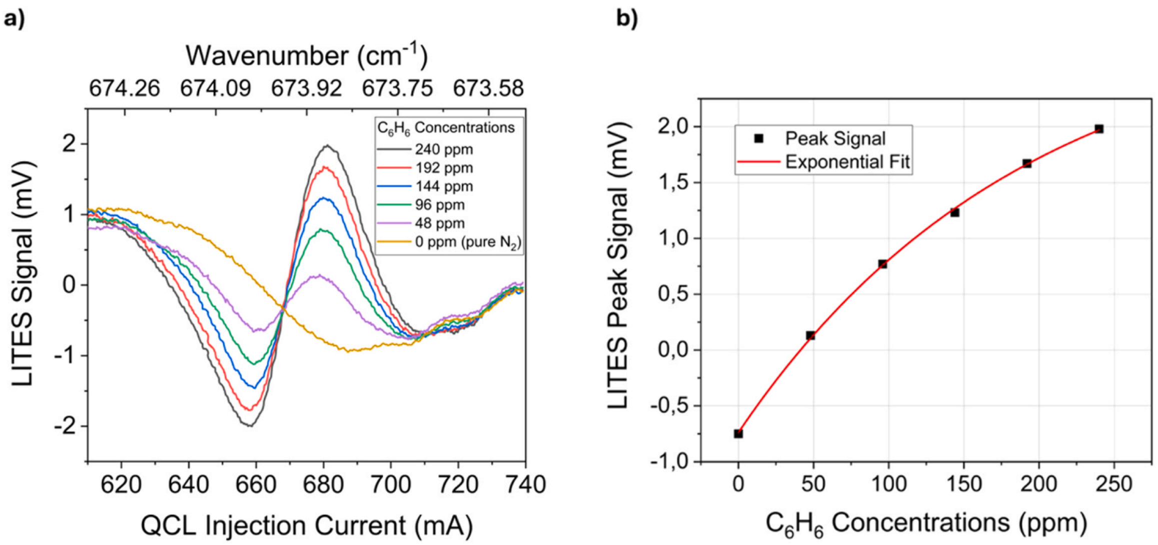

Fig. 7. (a) *2 f*-LITES spectral scans of the benzene absorption line at six benzene concentrations. The operating pressure was 700 Torr, and the modulation amplitude was 600 mV. (b) LITES peak signals as a function of the benzene concentration and the corresponding best exponential fit.

calibration curve at a given concentration. However, the MDL assessment requires an evaluation of the sensor response at low concentration ranges. In this range, the exponential trend can be linearized, leading to a sensitivity of 0.020 mV/ppm. A 1σ noise level of 0.012 mV was estimated at 100 ms lock-in integration time, corresponding to an MDL of 600 parts-per-billion (ppb). This demonstrates that our approach can detect benzene at sub-ppm levels under relatively compact conditions. Such performance can be compared with other spectroscopic techniques: benzene detection has indeed been reported using FTIR, achieving MDLs on the order of 100 ppb, but only with very long optical paths (up to 300 m) [37]. In comparison, our approach attains comparable sensitivity with a cell length of only 12 cm, which offers significant advantages in terms of compactness and cost-effectiveness. Even lower MDLs, down to a few ppb, have been demonstrated using QEPAS-based sensors [26,38]; however, these systems require careful consideration of the gas matrix in which benzene is contained, which can complicate their implementation.

7. Conclusion

This work introduces a novel approach for detecting broadband absorbers based on amplitude modulation, with respect to standard wavelength modulation and double-frequency detection. The selected sensing technique was LITES, using a long-wavelength QCL as the laser source, specifically designed to emit at 14.85 µm, resonant with the benzene absorption feature. A custom T-shaped QTF, with a resonance frequency of $f_0 = 12{,}460.7$ Hz, was used as a highly sensitive infrared photodetector. The LITES sensor was operated in two different detection modes: (i) amplitude modulation, and (ii) wavelength modulation. The AM mode enabled the accurate reconstruction of the spectral feature and retrieval of absorption parameters, yielding an absorption cross-section of $1.1\cdot10^{-1\ 7}$ cm^{2} and an absolute absorption coefficient of 270 cm^{-1} , in good agreement with theoretical values reported in the literature. The WM approach was also implemented but encountered challenges due to the requirement for high modulation depths, because of the large FWHM of the benzene absorption feature. This led to a distortion of the typical 2f-WM shape and the presence of a non-zero background even in the absence of the absorber. As a result, either post-processing subtraction was required, or a non-zero LITES signal at zero benzene concentration in the cell was accounted for, the latter being the approach adopted in this work. Consequently, the usual benefits of the 2f-WM method are compromised. A MDL of 1.6 ppm and 0.6 ppm was achieved with AM and WM approach, respectively, at a lock-in integration time of 100 ms. This difference is primarily attributed to the noise level, with AM exhibiting higher noise than WM.

Funding

The authors from Dipartimento Interuniversitario di Fisica di Bari acknowledge financial support from the project ENDOSCOPE – BaC Sapienza D3 4Health (no. B53C22006120001); and from the project National Quantum Science and Technology Institute (NQSTI) (no. PE00000023 - H93C22000670006). Qijie Wang acknowledge fundings from the A*STAR-MAECI project (no. R23I0IR041).

CRediT authorship contribution statement

Kumar Kinjalk: Writing – review & editing, Methodology. **Mongelli Lavinia:** Writing – original draft, Investigation, Formal analysis, Data curation. **Andrea Zifarelli:** Writing – original draft, Investigation, Formal analysis, Conceptualization. **Vincenzo Spagnolo:** Writing – review & editing, Supervision, Resources, Project administration, Methodology. **Qijie Wang:** Writing – review & editing, Supervision. **Pietro Patimisco:** Writing – review & editing, Supervision, Project administration, Formal analysis, Conceptualization. **Alexei Baranov:** Writing – review & editing, Resources, Methodology. **Angelo Sampaolo:** Writing – review & editing, Supervision, Methodology.

Declaration of Competing Interest

The authors declare that they have no known competing financial interests or personal relationships that could have appeared to influence the work reported in this paper.

Data availability

Data will be made available on request.

References

[1] J. Hodgkinson, R.P. Tatam, "Optical gas sensing: a review, Meas. Sci. Technol. 24 (1) (2013).
[2] J.M. Supplee, W. Lenth, E.A. Whittaker, "Theoretical description of frequency modulation and wavelength modulation spectroscopy, Appl. Opt. 33 (27) (1994) 6294–6302.
[3] P. Patimisco, A. Sampaolo, Y. Bidaux, A. Bismuto, M. Scott, J. Jiang, A. Muller, J. Faist, F.K. Tittel, V. Spagnolo, "Purely wavelength- and amplitude-modulated quartz-enhanced photoacoustic spectroscopy, Opt. Express 24 (23) (2016) 25943.
[4] G. Stewart, "Wavelength modulation spectroscopy with DFB lasers. Laser and Fiber Optic Gas Absorption Spectroscopy, Cambridge University Press, 2021, pp. 53–84.
[5] S. Schilt, L. Thévenaz, P. Robert, "Wavelength modulation spectroscopy: combined frequency and intensity laser modulation,", Appl. Opt. 42 (33) (2003) 6728.
[6] Y. Du, Z. Peng, Y. Ding, "Wavelength modulation spectroscopy for recovering absolute absorbance, Opt. Express 26 (7) (2018) 9263.
[7] K. Sun, X. Chao, R. Sur, J.B. Jeffries, R.K. Hanson, "Wavelength modulation diode laser absorption spectroscopy for high-pressure gas sensing, Appl. Phys. B 110 (4) (2013) 497–508.
[8] K. Duffin, A.J. McGettrick, W. Johnstone, G. Stewart, D.G. Moodie, "Tunable diode-laser spectroscopy with wavelength modulation: a calibration-free approach to the recovery of absolute gas absorption line shapes, J. Light. Technol. 25 (10) (2007) 3114–3125.
[9] T. Benoy, M. Lengden, G. Stewart, W. Johnstone, "Recovery of absorption line shapes with correction for the wavelength modulation characteristics of DFB lasers, IEEE Photonics J. 8 (3) (2016).
[10] H.L. Wang, L. Nie, J. Li, Y.F. Wang, G. Wang, J.H. Wang, Z.P. Hao, "Characterization and assessment of volatile organic compounds (VOCs) emissions from typical industries, Chin. Sci. Bull. 58 (7) (2013) 724–730.
[11] US Environmental Protection Agency, Technical overview of volatile organic compounds 2018.
[12] T.R.S. Hayden, G.B. Rieker, K. Sun, X. Chao, R. Sur, J.B. Jeffries, R.K. Hanson, "Large amplitude wavelength modulation spectroscopy for sensitive measurements of broad absorbers, Opt. Express 24 (24) (2016) 27910–27921.
[13] A. Behera, A. Wang, "Calibration-free wavelength modulation spectroscopy: symmetry approach and residual amplitude modulation normalization, Appl. Opt. 55 (16) (2016) 4446–4455.
[14] A.Lal Chakraborty, K. Ruxton, W. Johnstone, M. Lengden, K. Duffin, J. Reid, J. Shewchun, B.K. Garside, E.A. Ballik, "Elimination of residual amplitude modulation in tunable diode laser wavelength modulation spectroscopy using an optical fiber delay line, Opt. Express 17 (12) (2009) 9602–9607.
[15] M.T. Smith, "Advances in understanding benzene health effects and susceptibility, Annu. Rev. Public Health 31 (2010) 133–148.
[16] D. Pyatt, S. Hays, "A review of the potential association between childhood leukemia and benzene, Chem. Biol. Interact. 184 (1–2) (2010) 151–164.
[17] A. Tiwary, I. WilliamsAir pollution: measurement, modelling and mitigation, Fourth Edition 2019..
[18] S.Dello Russo, A. Zifarelli, P. Patimisco, A. Sampaolo, T. Wei, H. Wu, L. Dong, V. Spagnolo, "Light-induced thermo-elastic effect in quartz tuning forks exploited as a photodetector in gas absorption spectroscopy, Opt. Express 28 (13) (2020) 19074.
[19] Y. Ma, T. Liang, S. Qiao, X. Liu, Z. Lang, "Highly sensitive and fast hydrogen detection based on light-induced thermoelastic spectroscopy, Ultra Sci. 3 (2023).
[20] Y. Mi, Y. Ma, "Ultra-highly sensitive ammonia detection based on light-induced thermoelastic spectroscopy, Sensors 21 (13) (2021) 4548.
[21] Y. Ma, Y. He, P. Patimisco, A. Sampaolo, S. Qiao, X. Yu, F.K. Tittel, V. Spagnolo, "Ultra-high sensitive trace gas detection based on light-induced thermoelastic spectroscopy and a custom quartz tuning fork, Appl. Phys. Lett. 116 (1) (2020) 011103.
[22] B. Sun, P. Patimisco, A. Sampaolo, A. Zifarelli, V. Spagnolo, H. Wu, L. Dong, "Light-induced thermoelastic sensor for ppb-level H2S detection in a SF6 gas matrices exploiting a mini-multi-pass cell and quartz tuning fork photodetector, Photoacoustics 33 (2023) 100553.
[23] W. Chen, S. Qiao, Z. Lang, J. Jiang, Y. He, Y. Shi, Y. Ma, "Hollow-waveguide-based light-induced thermoelastic spectroscopy sensing, Opt. Lett. 48 (15) (2023) 3989.
[24] T. Wei, A. Zifarelli, S. Dello Russo, H. Wu, G. Menduni, P. Patimisco, A. Sampaolo, V. Spagnolo, L. Dong, "High and flat spectral responsivity of quartz tuning fork used as infrared photodetector in tunable diode laser spectroscopy, Appl. Phys. Rev. 8 (4) (2021) 041409.

[25] K. Kinjalk, D.A. Díaz-Thomas, Z. Loghmari, M. Bahriz, R. Teissier, A.N. Baranov, "InAs-based quantum cascade lasers with extremely low threshold, Photonics 9 (10) (2022) 747.

[26] K. Kinjalk, F. Paciolla, B. Sun, A. Zifarelli, G. Menduni, M. Giglio, H. Wu, L. Dong, D. Ayache, D. Pinto, A. Vicet, A. Baranov, P. Patimisco, A. Sampaolo, V. Spagnolo, "Highly selective and sensitive detection of volatile organic compounds using long wavelength InAs-based quantum cascade lasers through quartz-enhanced photoacoustic spectroscopy, Appl. Phys. Rev. 11 (2) (2024).

[27] I.E. Gordon, L.S. Rothman, R.J. Hargreaves, R. Hashemi, E.V. Karlovets, F. M. Skinner, E.K. Conway, C. Hill, R.V. Kochanov, Y. Tan, P. Wcisło, A.A. Finenko, K. Nelson, P.F. Bernath, M. Birk, V. Boudon, A. Campargue, K.V. Chance, A. Coustenis, B.J. Drouin, J.M. Flaud, R.R. Gamache, J.T. Hodges, D. Jacquemart, E.J. Mlawer, A.V. Nikitin, V.I. Perevalov, M. Rotger, J. Tennyson, G.C. Toon, H. Tran, V.G. Tyuterev, E.M. Adkins, A. Baker, A. Barbe, E. Canè, A.G. Császár, A. Dudaryonok, O. Egorov, A.J. Fleisher, H. Fleurbaey, A. Foltynowicz, T. Furtenbacher, J.J. Harrison, J.M. Hartmann, V.M. Horneman, X. Huang, T. Karman, J. Karns, S. Kassi, I. Kleiner, V. Kofman, F. Kwabia-Tchana, N. N. Lavrentieva, T.J. Lee, D.A. Long, A.A. Lukashevskaya, O.M. Lyulin, V. Y. Makhnev, W. Matt, S.T. Massie, M. Melosso, S.N. Mikhailenko, D. Mondelain, H. S.P. Müller, O.V. Naumenko, A. Perrin, O.L. Polyansky, E. Raddaoui, P.L. Raston, Z. D. Reed, M. Rey, C. Richard, R. Tóbiás, I. Sadiek, D.W. Schwenke, E. Starikova, K. Sung, F. Tamassia, S.A. Tashkun, J. Vander Auwera, I.A. Vasilenko, A.A. Vigasin, G.L. Villanueva, B. Vispoel, G. Wagner, A. Yachmenev, S.N. Yurchenko, "The HITRAN2020 molecular spectroscopic database, J. Quant. Spectrosc. Radiat. Transf. 277 (2022).

[28] Y. He, Y. Ma, Y. Tong, X. Yu, F.K. Tittel, "Ultra-high sensitive light-induced thermoelastic spectroscopy sensor with a high Q-factor quartz tuning fork and a multipass cell, Opt. Lett. 44 (8) (2019) 1904.

[29] H. Christina, N. Madhusudhan, "Effect of pressure broadening on molecular absorption cross sections in exoplanetary atmospheres, Mon. Not. R. Astron Soc. 458 (2) (2016) 1427–1449.

[30] W. Demtröder, Laser Spectroscopy. Vol. 1: Basic Principles, Springer-Verlag, 2008.

[31] L.S. Rothman, I.E. Gordon, A. Barbe, D.C. Benner, P.F. Bernath, M. Birk, V. Boudon, L.R. Brown, A. Campargue, J.P. Champion, K. Chance, L.H. Coudert, V. Dana, V. M. Devi, S. Fally, J.M. Flaud, R.R. Gamache, A. Goldman, D. Jacquemart, I. Kleiner, N. Lacome, W.J. Lafferty, J.Y. Mandin, S.T. Massie, S.N. Mikhailenko, C.E. Miller, N. Moazzen-Ahmadi, O.V. Naumenko, A.V. Nikitin, J. Orphal, V.I. Perevalov, A. Perrin, A. Predoi-Cross, C.P. Rinsland, M. Rotger, M. Šimečková, M.A.H. Smith, K. Sung, S.A. Tashkun, J. Tennyson, R.A. Toth, A.C. Vandaele, J. Vander Auwera, "The HITRAN 2008 molecular spectroscopic database, J. Quant. Spectrosc. Radiat. Transf. 110 (9–10) (2009) 533–572.

[32] T. Delahaye, R. Armante, N.A. Scott, N. Jacquinet-Husson, A. Chédin, L. Crépeau, C. Crevoisier, V. Douet, A. Perrin, A. Barbe, V. Boudon, A. Campargue, L. H. Coudert, V. Ebert, J.M. Flaud, R.R. Gamache, D. Jacquemart, A. Jolly, F. Kwabia Tchana, A. Kyuberis, G. Li, O.M. Lyulin, L. Manceron, S. Mikhailenko, N. Moazzen-Ahmadi, H.S.P. Müller, O.V. Naumenko, A. Nikitin, V.I. Perevalov, C. Richard, E. Starikova, S.A. Tashkun, V.G. Tyuterev, J. Vander Auwera, B. Vispoel, A. Yachmenev, S. Yurchenko, "The 2020 edition of the GEISA spectroscopic database, J. Mol. Spectrosc. 380 (2021) 111510.

[33] K. Ruxton, A.L. Chakraborty, W. Johnstone, M. Lengden, G. Stewart, K. Duffin, "Tunable diode laser spectroscopy with wavelength modulation: elimination of residual amplitude modulation in a phasor decomposition approach, Sens. Actuators B Chem. 150 (1) (2010) 367–375.

[34] L. Li, F. Liu, C. Wang, L. Chen, "Measurement and control of residual amplitude modulation in optical phase modulation, Rev. Sci. Instrum. 83 (4) (2012) 43111.

[35] E.A. Whittaker, H. Grebel, C.M. Shum, H. Lotem, "Reduction of residual amplitude modulation in frequency-modulation spectroscopy by using harmonic frequency modulation, JOSA B 5 (6) (1988) 1253–1256.

[36] G. Stewart, "Wavelength modulation spectroscopy with DFB lasers. Laser and Fiber Optic Gas Absorption Spectroscopy, Cambridge University Press, 2021, pp. 53–84.

[37] S.R. Schill, R.S. McEwan, R.C. Moffet, J.E. Marrero, C.P. MacDonald, E.D. Winegar, "Real-world application of open-path UV-DOAS, TDL, and FT-IR spectroscopy for air quality monitoring at industrial facilities, Spectroscopy 37 (2022) 18–22.

[38] D. Ayache, W. Trzpil, R. Rousseau, K. Kinjalk, R. Teissier, A.N. Baranov, M. Bahriz, A. Vicet, "Benzene sensing by quartz enhanced photoacoustic spectroscopy at 14.85 μm, Opt. Express 30 (4) (2022) 5531.

Andrea Zifarelli received the M.S. degree (cum laude) in Physics in 2018 from the University of Bari and his Ph.D. in Physics from the same institution in 2022. His research activities were mainly focused on the development of spectroscopic techniques based on laser absorption for the analysis of complex gas mixtures by employing quartz tuning forks as sensitive elements. This investigation was performed by using innovative laser sources as well as developing new algorithms for multivariate analysis approaches. Currently, he is Assistant Professor at University of Bari and his research activities are carried out at the PolySenSe Lab, joint-research laboratory between Technical University of Bari and THORLABS GmbH.

Lavinia Anna Mongelli obtained her M.S. degree in Physics in 2024 from the University of Bari. Currently she is research fellow at the Physics Department of the University of Bari, developing her research work at PolySense Lab, joint-research laboratory between Technical University of Bari and THORLABS GmbH. Her research activities are focused on the development of gas sensors based on optical spectroscopy for the detection of Volatile Organic Compounds and other gas species of interest for environmental and human health monitoring.

Alexei N. Baranov received the Ph.D. degree in 1985 from the IOFFE Institute (Leningrad, USSR) and his Habilitation Diploma in 1996 from the University of Montpellier 2, Montpellier, France. From 1978–1993, he was with the IOFFE Institute as a Junior Researcher, Researcher, and Senior Researcher. In 1993, he joined the National Center for Scientific Research (CNRS), France and is currently the Research Director of Institut d`Electronique et des Systèmes, University of Montpellier, Montpellier, France. He pioneered mid-infrared antimonide-based photonics, participating in the very first developments in this field and later directing this research with the IOFFE Institute and with Montpellier. He guided innovative investigations resulting in the demonstration of novel types of mid-infrared semiconductor lasers, light-emitting diodes and photodetectors. His current research activity is focused on physics and technology of InAs-based quantum cascade lasers and interband cascade lasers. His achievements in mid-infrared photonics have been recognized by the attribution of the Silver Medal of CNRS, one of the highest scientific awards in France. In 2017, he was elected Fellow of SPIE.

Pietro Patimisco obtained the Master degree in Physics (cum laude) in 2009 and the PhD Degree in Physics in 2013 from the University of Bari. Since 2023, he is an associate professor at the Physics Department of University of Bari. He was a visiting scientist in the Laser Science Group at Rice University in 2013 and 2014. The main scientific skills of Pietro Patimisco are related to the development of spectroscopic techniques for studying the light-matter interaction in the infrared range. Prof. Pietro Patimisco is co-founder of “PolySenSe Innovations”, a company devoted to the development of optical-based sensors.

Qijie Wang received the B.E. degree in electrical engineering from the University of Science and Technology of China (USTC), Hefei China, in 2001 graduating one year in advance; and the Ph.D degree in electrical and electronic engineering from Nanyang Technological University, Singapore, in 2005, with NTU and Singapore Millennium Foundation (SMF) scholarship. After completing his Ph.D, he obtained the 2005 SMF postdoctoral fellowship working in NTU. Then he joined School of Engineering and Applied Science, Harvard University, as a postdoctoral researcher in Jan. 2007. In October 2009, he was appointed as a joint Nanyang Assistant Professor at the School of Electrical and Electronic Engineering (EEE) and the School of Physical and Mathematical Sciences (SPMS). Since Sep. 2018, he has been promoted to tenured full professor in school of EEE and SPMS, NTU. He is an OSA (the Optical Society) Fellow.

Vincenzo Spagnolo received the degree (summa cum laude) and the PhD, both in physics, from University of Bari. He works as Full Professor of Applied Physics at the Technical University of Bari. In 2019, he become Vice-Rector of the Technical Uni versity of Bari, deputy to Technology Transfer. Since 2017, he is the director of the joint-research lab PolySense, created by THORLABS GmbH and Technical University of Bari, devoted to the development and implementation of novel gas sensing techniques and the realization of highly sensitive QEPAS trace- gas sensors. Prof. Vincenzo Spagnolo is co-founder of “PolySenSe Innovations”, a company devoted to the development of optical-based sensors.

Angelo Sampaolo obtained his Master degree in Physics in 2013 and the PhD Degree in Physics in 2017 from University of Bari. He was an associate researcher in the Laser Science Group at Rice University from 2014 to 2016 and associate researcher at Shanxi University since 2018. Since 2023, he is Associate Professor at Polytechnic of Bari. His research activity has focused on the development of innovative techniques in trace gas sensing, based on Quartz-Enhanced Photoacoustic Spectroscopy and covering the full spectral range from near-IR to THz. Prof. Angelo Sampaolo is co-founder and CEO of “PolySenSe Innovations”, a company devoted to the development of optical-based sensors.